

# Finite Random Domino Automaton

Mariusz Bialecki\*

*Institute of Geophysics, Polish Academy of Sciences  
ul. Ks. Janusza 64, 01-452 Warszawa, Poland*

(Dated: September 11, 2018)

Finite version of Random Domino Automaton (FRDA) - recently proposed in [1] as a toy model of earthquakes - is investigated. Respective set of equations describing stationary state of the FRDA is derived and compared with infinite case. It is shown that for the system of big size, these equations are coincident with RDA equations. We demonstrate a non-existence of exact equations for size  $N \geq 5$  and propose appropriate approximations, the quality of which is studied in examples obtained within Markov chains framework.

We derive several exact formulas describing properties of the automaton, including time aspects. In particular, a way to achieve a quasi-periodic like behaviour of RDA is presented. Thus, based on the same microscopic rule - which produces exponential and inverse-power like distributions - we extend applicability of the model to quasi-periodic phenomena.

PACS numbers: 45.70.Ht (Avalanches), 02.50.Ga (Markov processes), 91.30.Px (Earthquakes)

Keywords: stochastic cellular automata, avalanches, exact solutions, toy models of earthquakes, forest-fire models, Markov chains

## I. INTRODUCTION

The Random Domino Automaton, proposed in [1], is a stochastic cellular automaton with avalanches. It was introduced as a toy model of earthquakes, but can be also regarded as an substantial extension of 1-D forest-fire model proposed by Drossel and Schwabl [2–4].

The remarkable feature of the RDA is the explicit one-to-one relation between details of the dynamical rules of the automaton (represented by rebound parameters  $\mu_i/\nu$  defined in cited article and also below) and the produced stationary distribution  $n_i$  of clusters of size  $i$ , which implies distribution of avalanches. It is already shown how to reconstruct details of the "microscopic" dynamics from the observed "macroscopic" behaviour of the system [1, 5].

As a field of application of RDA we studied a possibility of constructing the Ito equation from a given time series and - in a broader sense - applicability of Ito equation as a model of natural phenomena. For RDA - which plays a role of a fully controlled stochastic natural phenomenon - the relevant Ito equation can be constructed in two ways: derived directly from equations and by histogram method from generated time series. Then these two results are compared and investigated in [6, 7].

Note that the set of equations of the RDA in a special limit case reduces to the recurrence, which leads to known integer sequence - the Motzkin numbers, which establishes a new, remarkable link between the combinatorial object and the stochastic cellular automaton [8].

In the present paper a finite version of Random Domino Automaton is investigated. The mathematical formulation in finite case is precise and the presented

results clarify which formulas are exact and allow to estimate approximations we impose in infinite case presented in [1]. We also show, that equations of finite RDA can reproduce results of [1], when size  $N$  of the system is increasing and distributions satisfy an additional assumption ( $n_i \rightarrow 0$  for big  $i$ ).

On the other hand, a time evolution of Finite RDA can exhibit a periodic-like behaviour (the assumption  $n_i \rightarrow 0$  for big  $i$  is violated), which is a novel property. Thus, based on the same microscopic rules, depending on a choice of parameters of the model, a wide range of properties is possible to obtain. In particular, such behaviour is interesting in the context of recurrence parameters of earthquakes (see e.g. [9, 10]). For other simple periodic-like models, see [11, 12].

The finite case makes an opportunity to employ Markov chains techniques to analyse RDA. Investigating the automaton in Markov chains framework we arrive at several novel conclusions, in particular related to expected waiting times for some specified behaviour.

This article completes and substantially extends previous studies of RDA on the level of mathematical structure. We analyse properties of the automaton related to time evolution and others, as a preparation for further prospective comparisons with natural phenomena, including earthquakes. A matter of adjusting the model to the real data is left for the forthcoming paper.

The plan of the article is as follows. Mimicking [1] in Section II we define the finite RDA. In Section III we derive respective equations for finite RDA. In Section IV we will specify them for some chosen cases. In Section V we will shortly describe Markov chains setting and describe time aspects of FRDA. Several examples are presented in Section VI. The last Section VII contain conclusions and remarks. In the Appendix we show non existence of exact equations for RDA as well as present supplementary formulas and Table XIV displaying all states of RDA of size  $N = 10$ .

---

\*Electronic address: bialecki@igf.edu.pl



**Loss.** Two ways contribute: joining a cluster with another one and removing a cluster due to avalanche.

Joining of two clusters can occur if there exists an empty cluster of length 1 between them. The exception is when the empty 1-cluster is the only one empty cluster, and the system consists of a single cluster of length  $N - 1$ . Hence, the probability of joining two clusters is

$$\sim \nu \left( \frac{n_1^0}{N} - n_{N-1} \right). \quad (7)$$

The probability of avalanche is just

$$\sim \sum_{i=1}^N \mu_i \frac{n_i i}{N}. \quad (8)$$

Gathering these terms one obtains equation for balance of the total number of clusters  $n$

$$N(1 - \rho) - \sum_{i=1}^N \frac{\mu_i}{\nu} n_i i + n_{N-1} = 2n_R. \quad (9)$$

Again we emphasise that the above result is exact – no correlations were neglected. Finite size of the system reflects in the appearance of  $(2n_R - n_{N-1})$  instead of  $2n$  in the respective formula in [1].

### C. Balance of $n_i$ s

**Loss.** There are two modes.

(a) Enlarging - an empty cluster on the edge of an  $i$ -cluster becomes occupied. There are two such empty clusters except for the case when system contains a single cluster of length  $N - 1$ . Hence, the respective rates are

$$\sim 2\nu \frac{n_i}{N} \quad i = 1, \dots, N - 2, \quad (10)$$

$$\sim \nu \frac{n_{N-1}}{N} \quad i = N - 1. \quad (11)$$

(b) Relaxation rate for any  $i = 1, \dots, N$  is given by

$$\sim \mu_i \frac{in_i}{N}. \quad (12)$$

**Gain.** Again, there are two modes.

(a) Enlarging. For  $N \geq 3$ , there are following rates depending on the size  $i$  of the cluster

$$\sim \nu(1 - \rho) - 2\nu \frac{n_R}{N} + \nu \frac{n_1^0}{N}, \quad i = 1, \quad (13)$$

$$\sim 2\nu \frac{n_{i-1}}{N} \alpha_{i-1}^E \quad 2 \leq i \leq N - 1, \quad (14)$$

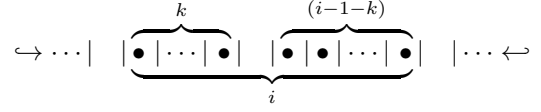
$$\sim \nu \frac{n_{N-1}}{N}, \quad i = N, \quad (15)$$

where  $\alpha_E(i)$  is a probability that the size of empty cluster adjacent to the  $i$ -cluster is bigger than 1. It is clear that

$$\alpha_{N-2}^E = 1 \quad \text{and} \quad \alpha_{N-1}^E = 0. \quad (16)$$

Formula (15) does not have a factor 2, because there is only one empty cluster (of size 1).

(b) Merger of two clusters up to the cluster of size  $i$ . Two clusters: one of size  $k \in \{1, 2, \dots, (i - 2)\}$  and the other of size  $((i - 1) - k)$  will be combined if the ball fills an empty cell between them.



The probability is proportional to the number of empty 1-clusters between  $k$ -cluster and  $(i - 1 - k)$ -cluster,

$$\sim \nu \frac{n_1^0}{N} \gamma_i^E \quad 3 \leq i \leq N - 1, \quad (17)$$

where  $\gamma_i^E$  is a probability of such merger. For  $i = N$  there is a single cluster in the lattice (there are no two clusters to merge) - filling the gap between ends of  $(N - 1)$ -cluster is already considered in (a).

Gathering the terms, one obtains

$$n_1 = \frac{1}{\frac{\mu_1}{\nu} + 2} (N(1 - \rho) - 2n_R + n_1^0), \quad (18)$$

$$n_2 = \frac{1}{2\frac{\mu_2}{\nu} + 2} 2n_1 \alpha_1^E, \quad (19)$$

$$n_i = \frac{1}{\frac{\mu_i}{\nu} i + 2} (2n_{i-1} \alpha_{i-1}^E + n_1^0 \gamma_i^E), \quad (20)$$

$$n_{N-1} = \frac{1}{\frac{\mu_{N-1}}{\nu} (N - 1) + 1} (2n_{N-2} + n_1^0 \gamma_{N-1}^E), \quad (21)$$

$$n_N = \frac{1}{\frac{\mu_N}{\nu} N} n_{N-1}, \quad (22)$$

where  $3 \leq i \leq (N - 2)$ .

The last equation (22) has simple explanation. The state with all cells being occupied (corresponding to  $n_N$ ) can be achieved only from the state with a single empty cell (corresponding to  $n_{N-1}$ ) with probability  $\nu(1/N)$ . On the other hand, the automaton leaves the state with all cells being occupied with probability  $\mu_N$ .

Note that equations (18) and (22) are exact. Correlations in the systems reflect in appearing of multipliers  $\alpha_i^E$  and  $\gamma_i^E$ . Their values depends on possible configurations of states of the automaton. As shown in the Appendix, for  $N \geq 5$  exact formulas for  $\alpha_i^E$  and  $\gamma_i^E$  as functions of  $n_i$ s do not exist. Hence, it is necessary to propose approximated formulas.

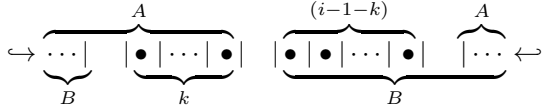
A mean field type approximation for  $\alpha_i^E$  is

$$\alpha_i^E \approx \alpha_i^A = \left( 1 - \frac{n_1^0}{\sum_{k=1}^{N-i} n_k^0} \right). \quad (23)$$

For a given cluster of size  $i$ , the probability of appearance of an empty cluster of size 1 is calculated as proportional to the number of empty 1-clusters divided by the sum of the numbers of all empty clusters with size not exceeding  $N - 1$ , because there is no room for larger.

When merger of two clusters up to a cluster of size  $i$  is considered, the room denoted by  $A$  is of size  $(N - 2 - (i -$

$1 - k$ ) and the room denoted by  $B$  is of size  $(N - 2 - k)$  - see a diagram below.



Hence a mean field type approximation for  $\gamma_i^E$  is of the form

$$\gamma_i^E \approx \gamma_i^A = \sum_{k=1}^{i-2} \left( \frac{n_k}{\sum_{j=1}^{N-(i-1-k+2)} n_j} \cdot \frac{n_{i-1-k}}{\sum_{j=1}^{N-(k+2)} n_j} \right). \quad (24)$$

It is also instructive to consider another approximation

$$\gamma_i^E \approx \gamma_i^{AR} = \sum_{k=1}^{i-2} \left( \frac{n_k}{n_R} \cdot \frac{n_{i-1-k}}{n_R} \right). \quad (25)$$

Section VI contains quantitative estimation of proposed approximations. Comparison of this approximation with exact results for small sizes  $N$  is discussed in Section VII.

#### D. Thermodynamic limit

In the paper [1] an assumption of independence of clusters was considered. To have it adequate, it is required that there are no limitations in space, like those encountered when formulas (23) and (24) were considered. For systems that are big enough, i.e., when  $N \rightarrow \infty$ , an empty cluster adjacent to a given  $i$ -cluster can be of any size, and thus

$$\alpha_i^E \approx \alpha = \left( 1 - \frac{n_1^0}{\sum_{k=1}^{\infty} n_k^0} \right) = \left( 1 - \frac{n_1^0}{n} \right). \quad (26)$$

This is consistent with the requirement that  $n_i \rightarrow 0$  when  $i \rightarrow \infty$ , which is required to have moments of the  $n_i$ s convergent. Similarly,

$$\gamma_i^E \approx \gamma(i) = \sum_{k=1}^{i-2} \left( \frac{n_k}{n} \cdot \frac{n_{i-1-k}}{n} \right). \quad (27)$$

These formulas substituted into (18)-(20) give the respective set of equations considered in [1]. The same reasoning can be applied to balance equations. The form of equation (4) is left unchanged under the limit. For equation (9),  $(2n_R - n_{N-1}) \rightarrow 2n$ , and it becomes of the form presented in [1].

#### IV. SPECIAL CASES

For fixed form of rebound parameters equations describing the automaton can be written in more specific

form. This is the case for balance equations (4) and (9), as well as for formulas for average cluster size

$$\langle i \rangle = \frac{\sum_{i=1}^N n_i i}{\sum_{i=1}^N n_i} = \frac{N\rho}{n_R + n_N} \quad (28)$$

and average avalanche size

$$\langle w \rangle = \frac{\sum_{i=1}^N \mu_i n_i i^2}{\sum_{i=1}^N \mu_i n_i i}. \quad (29)$$

We emphasize, these formulas are exact – correlations are encountered. We consider three special cases investigated in detail and illustrated by examples below.

##### A. $\mu = const.$

For  $\mu = const.$  and  $\nu = const.$  equation (4) is of the form

$$(1 - \rho) = \frac{1}{N} \frac{\mu}{\nu} \sum_{i=1}^N n_i i^2. \quad (30)$$

and equation (9)

$$N(1 - \rho(1 + \frac{\mu}{\nu})) + n_{N-1} = 2n_R. \quad (31)$$

Also formulas for  $\langle i \rangle$  and  $\langle w \rangle$  are simplified only a little.

##### B. $\mu(i) = \delta/i$ where $\theta = \delta/\nu = const.$

Equation (4) is of the form

$$(1 - \rho) = \theta\rho, \quad (32)$$

hence the density is given by remarkably neat (and exact) formula

$$\rho = \frac{1}{1 + \theta}. \quad (33)$$

Note that there is no dependence on the size of the system  $N$ ; for  $N \rightarrow \infty$  it remains the same.

Equation (9) can be written as

$$N \frac{\theta}{1 + \theta} = (2 + \theta)n_R, \quad (34)$$

where we use equations (22) and (33). Hence the formula for  $n_R$  is of the form

$$n_R = N \frac{\theta}{(\theta + 1)(\theta + 2)} \quad (35)$$

in direct analogy with  $n$  in  $N \rightarrow \infty$  case [1]. Thus,  $n_R$  plays the role of  $n$ , as indicated also in balance of  $n_1$  equation (18). The formula for  $n$  is

$$n = n_R + n_N = N \frac{\theta(1 + \varepsilon)}{(\theta + 1)(\theta + 2)} \quad \text{where} \quad \varepsilon = \frac{n_N}{n_R}. \quad (36)$$



$$\mathbf{P} = \frac{1}{5} \begin{pmatrix} 5 - 5\nu & 5\nu & 0 & 0 & 0 & 0 & 0 & 0 \\ \mu_1 & 5 - \mu_1 - 4\nu & 2\nu & 2\nu & 0 & 0 & 0 & 0 \\ 2\mu_2 & 0 & 5 - 2\mu_2 - 3\nu & 0 & 2\nu & \nu & 0 & 0 \\ 0 & 2\mu_1 & 0 & 5 - 2\mu_1 - 3\nu & \nu & 2\nu & 0 & 0 \\ 3\mu_3 & 0 & 0 & 0 & 5 - 3\mu_3 - 2\nu & 0 & 2\nu & 0 \\ 0 & 2\mu_2 & \mu_1 & 0 & 0 & 5 - 2\mu_2 - \mu_1 - 2\nu & 2\nu & 0 \\ 4\mu_4 & 0 & 0 & 0 & 0 & 0 & 0 & 5 - 4\mu_4 - \nu \\ 5\mu_5 & 0 & 0 & 0 & 0 & 0 & 0 & 5 - 5\mu_5 \end{pmatrix} \quad (46)$$

Stationary distribution is given by

$$v \cdot P = v. \quad (47)$$

The number of states increase rapidly with  $N$ : for  $N = 6$  there are 14 states, for  $N = 7$  there are 20 states and for  $N = 10$  there are 108 states. The number of states for any  $N$  is bigger than  $2^N/N$ , because translational symmetry of states is at most  $N$ , but always there are states with smaller symmetry, like empty state and fully occupied state. Thus practical usage of Markov chain settings for calculations is rather limited. This is one of the reasons for developing more "handy" framework, like presented in [1] and here. On the other hand, Markov chains can be used for illustrations and justifications of some properties, as presented below.

### B. Expected time of return

As system evolves, it hits a given state many times. Here we consider expected value of the time of return from state with density  $\rho = 0$  to itself and next from the state with  $\rho = 1$  to itself.

Starting from state 1 (state with  $\rho = 0$ ) the next state (different from state 1) contains a single 1-cluster only. This state - denoted by label 2 - has density  $\rho = 1/N$ . Expected time for this change is  $1/\nu$ .

Let  $\tau_i$  be the expected time to hit state 1 starting in state  $i$ . Then  $\tau_1 = 0$  and for  $i \neq 1$

$$\begin{aligned} \tau_i &= \mathbb{E}(\text{time to hit 1} \mid \text{start in } i) \\ &= 1 + \sum_k p_{ik} \mathbb{E}(1|k) = 1 + \sum_k p_{ik} \tau_k, \end{aligned} \quad (48)$$

where  $\mathbb{E}(1|k) = \mathbb{E}(\text{time to hit 1} \mid \text{start in } k)$ . After solving this system of equations, the return time is

$$t_{1 \rightarrow 1} = 1/\nu + \tau_2. \quad (49)$$

Similarly, for state with  $\rho = 1$  (state  $L$ ) the next state (different from state  $L$ ) is the empty state (with  $\rho = 0$ ) and

$$t_{L \rightarrow L} = 1/\mu_N + \hat{\tau}_1, \quad (50)$$

where  $\hat{\tau}_1$  is the expected time to hit state  $L$  starting in state 1. The respective equation to determine  $\hat{\tau}_i$  for  $i \neq L$  reads

$$\hat{\tau}_i = 1 + \sum_k p_{ik} \hat{\tau}_k, \quad (51)$$

and obviously  $\hat{\tau}_L = 0$ .

Note that the expected time  $t_{L \rightarrow L}$  is equal to expected time of return from state 1 to state 1 through state  $L$ :

$$t_{L \rightarrow L} = t_{1 \rightarrow L \rightarrow 1}. \quad (52)$$

The expected time between two consecutive avalanches is

$$t_{av} = \frac{\langle w \rangle + 1}{1 - P_r}, \quad (53)$$

where  $P_r$  is the probability that the incoming ball is rebounded both form empty or occupied cell:

$$P_r = (1 - \rho)(1 - \nu) + \frac{1}{N} \sum_{i=1}^N n_i i (1 - \mu_i). \quad (54)$$

Note that  $(1 - P_r)$  is equal to the sum of probability of triggering an avalanche and probability that an empty cell becomes occupied, hence

$$P_r + \frac{1}{N} \sum_{i=1}^N \mu_i n_i i + (1 - \rho)\nu = 1. \quad (55)$$

Formula (53) can be derived as follows. In time between two consecutive avalanches, on average,  $(t_{av}(1 - P_r) - 1)$  cells become occupied in the system - it receives one ball per a time step, part of them are rebounded and one ball triggers the avalanche. An avalanche is reducing the

probability of	value
rebound - occupied cell	$\frac{1}{N} \sum_{i=1}^N n_i i (1 - \mu_i)$
rebound - empty cell	$(1 - \rho)(1 - \nu)$
occupation of empty cell	$(1 - \rho)\nu$
triggering an avalanche	$\frac{1}{N} \sum_{i=1}^N \mu_i n_i i$

TABLE III: Probabilities of all four possibilities occurring in a single time step during evolution of the automaton.

number of occupied cells by  $\langle w \rangle$ . These two quantities compensate each other, giving (53).

On the other hand, the expected time between two consecutive avalanches is equal to the inverse of the probability of triggering an avalanche

$$t_{av} = \left( \frac{1}{N} \sum_{i=1}^N \mu_i n_i i \right)^{-1}. \quad (56)$$

Both expressions given in (53) and (56) are equal to each other.

### C. Frequency distribution of avalanches

The probability of states obtained from condition (47) allows to determine the distribution of frequency of avalanches. The frequency  $f_i$  of the avalanche of size  $i$  is given by the sum of products of probabilities  $v_k$  of state  $k$  and respective transition probability  $p_{kj}$  to the appropriate states  $j$  for all states that transition  $k \rightarrow j$  produce the avalanche of size  $i$ .

For example, for  $N = 5$ , as can be seen in Table II, transitions  $2 \rightarrow 1$ ,  $4 \rightarrow 2$  and  $6 \rightarrow 3$  result in an avalanche of size 1, transitions  $3 \rightarrow 1$  and  $6 \rightarrow 2$  give an avalanche of size 2, transition  $5 \rightarrow 1$  of size 3,  $7 \rightarrow 1$  of size 4 and  $8 \rightarrow 1$  of size 5. Hence

$$f_1 = v_2 \mu_1 / 5 + v_4 2 \mu_1 / 5 + v_6 \mu_1 / 5, \quad (57)$$

$$f_2 = v_3 2 \mu_2 / 5 + v_6 2 \mu_2 / 5, \quad (58)$$

$$f_3 = v_5 3 \mu_3 / 5, \quad (59)$$

$$f_4 = v_7 4 \mu_4 / 5, \quad (60)$$

$$f_5 = v_8 \mu_5, \quad (61)$$

where respective  $p_{kj}$  are taken from transition matrix (46).

The average time  $t_i$  between two avalanches of size  $i$  is given by

$$t_i = 1/f_i, \quad (62)$$

in particular, for a maximum size  $N$

$$t_{L \rightarrow L} = t_N. \quad (63)$$

The average time between (any) consecutive avalanches given by formula (56) may be also calculated as

$$t_{av} = \left( \sum_{i=1}^N t_i^{-1} \right)^{-1}, \quad (64)$$

because the probability of avalanche of any size is just a sum of probabilities of all possible avalanches. In this way one can calculate also average time between any two consecutive avalanches of prescribed size - for example, size 4 and 5 (or any other subset of possible sizes).

## VI. EXAMPLES

Below we present several examples to illustrate properties of finite RDA as well as to demonstrate application of the schemes outlined above.

### A. $N = 3$

This is the simplest non-trivial, worm-up example. For  $N = 3$  the general results - i.e., for arbitrary  $\mu_1$ ,  $\mu_2$ ,  $\mu_3$  and  $\nu$  - can be calculated explicitly. Usage of equations (18)-(22) leads to exact results as presented below (see Appendix). The same can be also obtained from Markov chains framework. Equations (4), (9), and (22) give

$$n_1 = 3 \left( \frac{\mu_2}{\nu} + \frac{1}{2} \right) / D, \quad (65)$$

$$n_2 = 3/D, \quad (66)$$

$$n_3 = \left( \frac{\nu}{\mu_3} \right) / D, \quad (67)$$

where

$$D = \frac{11}{2} + \frac{\mu_1}{2\nu} + 5 \frac{\mu_2}{\nu} + \frac{\mu_1 \mu_2}{\nu^2} + \frac{\nu}{\mu_3}.$$

From inspecting of Table I it is evident that  $n_1^0 = n_2$ ,  $n_2^0 = n_1$  and  $n_3^0 = 1 - n_1 - n_2 - n_3$  (all possibilities sum up to 1), hence

$$n_3^0 = \left( 1 + \frac{\mu_1}{2\nu} + 2 \frac{\mu_2}{\nu} + \frac{\mu_1 \mu_2}{\nu^2} \right) / D. \quad (68)$$

General formulas for expected times of return are

$$t_{1 \rightarrow 1} = \frac{1}{\nu} \left( 1 + \frac{2\nu^2 + 9\mu_3\nu + 6\mu_2\mu_3}{\mu_3(\mu_1 + 2\nu)(2\mu_2 + \nu)} \right), \quad (69)$$

$$t_{L \rightarrow L} = \frac{1}{\nu} \left( \frac{\nu}{\mu_3} + \frac{11}{2} + \frac{\mu_1}{2\nu} + 5 \frac{\mu_2}{\nu} + \frac{\mu_1 \mu_2}{\nu^2} \right). \quad (70)$$

The ratio  $t_{L \rightarrow L} / t_{1 \rightarrow 1}$  is

$$t_{L \rightarrow L} / t_{1 \rightarrow 1} = \frac{1}{2} \left( \frac{\mu_1}{\nu} + 2 \right) \left( \frac{2\mu_2}{\nu} + 1 \right). \quad (71)$$

Note that it does not depend on  $\mu_3$ . If the probability of triggering an avalanche of size 1 and 2 is small comparing to the probability of occupation of an empty cell (i.e.,  $\mu_1/\nu \approx 0$  and  $\mu_2/\nu \approx 0$ ) then  $t_{L \rightarrow L} \approx t_{1 \rightarrow 1}$ . The next stage after the lattice is fully occupied is the empty state; hence, if these two average waiting times are comparable, then they occur with comparable frequency. That means quasi-periodic like behaviour of the system: within average time  $11/2\nu$  the lattice become fully occupied, then the triggering of an avalanche of maximal size  $N$  occurs with average waiting time  $1/\mu_3$ . The same can be observed for bigger sizes  $N$ .

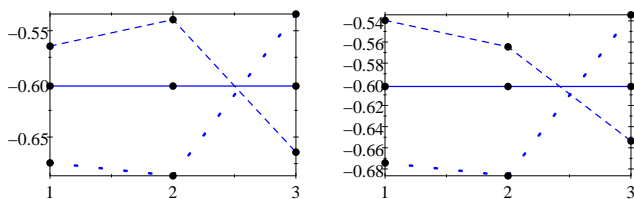


FIG. 1: Plot of the  $\text{Log}_{10}$  of  $n_i$ s (left) and  $n_i^0$ s (right) vs.  $i$  for  $N = 3$  in three cases:  $\mu_i = \text{const.}$  (dashed line),  $\mu_i = \delta/i$  (solid line) and  $\mu_i = \sigma/i^2$  (dotted line). Rebound parameters are chosen to have density  $\rho = 1/2$  in all cases (see main text for respective values).

	$\mu_i = \text{const.}$	$\mu_i = \delta/i$	$\mu_i = \sigma/i^2$
$\langle i \rangle$	1.9281668	2	2.1134407
$\langle w \rangle$	2.2516538	2	1.7226121

TABLE IV: Average cluster size  $\langle i \rangle$  and average avalanche size  $\langle w \rangle$  for three different rebound parameters. Density  $\rho = 1/2$ , the size of the lattice  $N = 3$ .

Figure 1 and Table IV present examples of three types of dependence of rebound parameters on size  $i$  of clusters considered in Section IV, each having the same density  $\rho = 1/2$  (with 8 digits accuracy). To obtain this density we put for these three cases  $\mu/\nu = 0.444118$  ( $\mu = 0.444118$ ,  $\nu = 1$ ),  $\theta = 1$  ( $\delta = 1$ ,  $\nu = 1$ ) and  $\chi = 2.113440690$  ( $\eta = 1$ ,  $\nu = 1/2.113440690$ ) respectively. As seen from Figure 1 it is possible to obtain flat distribution for  $\mu_i = \delta/i$  – on that background, differences between the cases are clearly visible:  $\mu_i = \text{const.}$  discriminate the existence of big clusters fostering big avalanches; the opposite is for  $\mu_i = \sigma/i^2$ . Average cluster size and avalanche size data presented in Table IV confirm this conclusion.

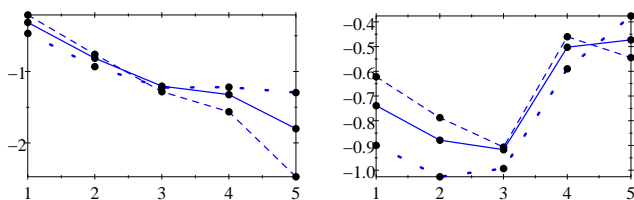


FIG. 2: Plot of the  $\text{Log}_{10}$  of  $n_i$ s (left) and  $n_i^0$ s (right) versus  $i$  for  $N = 5$  in three cases:  $\mu_i = \text{const.}$  (dashed line),  $\mu_i = \delta/i$  (solid line) and  $\mu_i = \sigma/i^2$  (dotted line). Rebound parameters are chosen to have density  $\rho = 1/4$  in all cases (see main text for respective values).

	$\mu_i = \text{const.}$	$\mu_i = \delta/i$	$\mu_i = \sigma/i^2$
$\langle i \rangle$	1.427017126	1.632218845	1.985611461
$\langle w \rangle$	1.845355789	1.632218845	1.41360643

TABLE V: Average cluster size  $\langle i \rangle$  and average avalanche size  $\langle w \rangle$  for three different rebound parameters. Density  $\rho = 1/4$ , the size of the lattice  $N = 5$ .

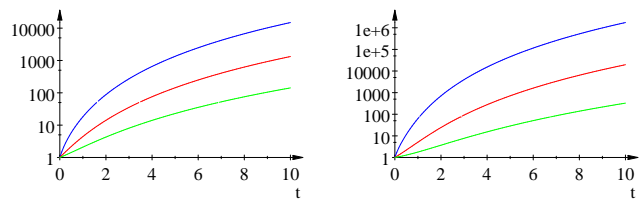


FIG. 3: Ratio of return times  $t_{L \rightarrow L}/t_{1 \rightarrow 1}$  for  $N=5$  (left) and  $N=7$  (right) for three cases:  $\mu_i = \text{const.}$  (top),  $\mu_i = \delta/i$  (middle) and  $\mu_i = \eta/i^2$  (bottom). Parameter  $t$  is equal to  $\mu/\nu$ ,  $\delta/\nu$  and  $\eta/\nu$  respectively.

## B. $N = 5$

For  $N = 5$  it is impossible to write down exact equations (18)-(22) depending on values of  $n_i$ s only – see Appendix for details. The case can be solved as a Markov process, but obtained general formulas are relatively complicated.

In this example we investigate properties of the system with density  $\rho = 1/4$ . Figure 2 and Table V compare results in three cases:  $\mu/\nu = 16257/10000$  the density  $\rho = 0.2500003184$ ; for  $\theta = 3$  the density  $\rho = 0.25$  exactly; and  $\chi = 5.95682$  gives the density  $\rho = 0.2500004527$ .

General expressions for return times  $t_{1 \rightarrow 1}$  and  $t_{L \rightarrow L}$  as well as their ratio (presented in Appendix) are relatively complex. Note that the return times – except of the dependence on  $t$  – are proportional to  $1/\nu$ . Below we specify the ratio  $t_{L \rightarrow L}/t_{1 \rightarrow 1}$  in three cases: for  $\mu_i = \text{const.}$ , where  $t = \mu/\nu$ , it is equal to

$$\frac{24t^6 + 154t^5 + 413t^4 + 586t^3 + 467t^2 + 182t + 24}{24t^2 + 54t + 24}, \quad (72)$$

for  $\mu_i = \delta/i$ , where  $\delta = \text{const}$  and  $t = \delta/\nu$ , it is equal to

$$\frac{4t^6 + 40t^5 + 169t^4 + 395t^3 + 550t^2 + 432t + 144}{56t^2 + 192t + 144}, \quad (73)$$

and for  $\mu_i = \sigma/i^2$ , where  $\sigma = \text{const}$  and  $t = \sigma/\nu$ , is

$$\frac{2t^6 + 39t^5 + 304t^4 + 1232t^3 + 2840t^2 + 3744t + 2304}{496t^2 + 2208t + 2304}. \quad (74)$$

In each case the ratio is a rational function of  $t$ , which is equal to 1 for  $t = 0$  and asymptotically  $\sim t^4$  for  $t \rightarrow \infty$ . A generalisation of this observation is a Conjecture formulated in Section VII. A comparison of these ratios is presented in left part of Figure 3. Table VI shows that for the cases discussed above with average density

	$\mu_i = \text{const.}$	$\mu_i = \delta/i$	$\mu_i = \sigma/i^2$
$R = t_{L \rightarrow L}/t_{1 \rightarrow 1}$	$\approx 52.212$	$\approx 35.441$	$\approx 34.801$

TABLE VI: Coefficient  $R = t_{L \rightarrow L}/t_{1 \rightarrow 1}$  for three different rebound parameters (see main text for details). Density for all cases  $\rho = 1/4$ , the size of the lattice  $N = 5$ .



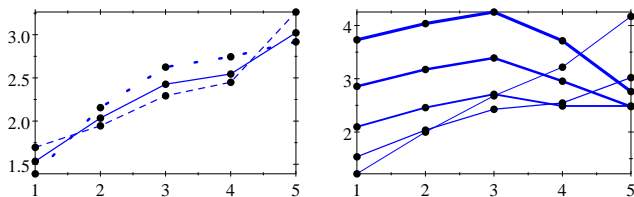


FIG. 4: **Left.** Plot of  $\text{Log}_{10}$  of  $t_{is}$  vs.  $i$  for three rebound parameters for fixed density  $\rho = 1/4$  for  $N = 5$ . Three cases:  $\mu_i = \text{const.}$  (dashed line),  $\mu_i = \delta/i$  (solid line) and  $\mu_i = \sigma/i^2$  (dotted line). Rebound parameters are chosen to have density  $\rho = 1/4$  in all cases (see main text for respective values). **Right.** Plot of  $\text{Log}_{10}$  of  $t_{is}$  versus  $i$  for various densities for rebound parameter of the form  $\mu_i = \delta/i$  for  $N = 5$ . Densities are chosen as  $\frac{1}{10}, \frac{1}{4}, \frac{1}{2}, \frac{3}{4}, \frac{9}{10}$ ; thinner line corresponds to smaller density.

$\rho = 1/4$  the highest value of  $R$  is for  $\mu_i = \text{const.}$  and the smallest for  $\mu_i = \sigma/i^2$  (not much different from the value for  $\mu_i = \delta/i$ ).

Average waiting times  $t_i$  for avalanche of size  $i$  can be also found. For example for  $\mu_i = \delta/i$ , where  $\delta = \text{const.}$ , they are presented in the Appendix (equations (81)-(85)). The average time between any two consecutive avalanches is

$$t_{av} = \frac{4t^5 + 48t^4 + 237t^3 + 603t^2 + 762t + 360}{\nu t(4t^4 + 36t^3 + 121t^2 + 168t + 72)}, \quad (75)$$

where  $t = \delta/\nu$ . All these quantities are proportional to  $1/\nu$ . Figure 4 in the left panel presents waiting times  $t_i$  in for fixed density  $\rho = 1/4$  in three cases mentioned above. There are no big differences both in character of dependence of  $t_i$  on  $i$  and also values of  $t_{av}$  do not differ much: for  $\mu_i = \text{const.}$  average time is  $t_{av} \approx 24.60$ , for  $\mu_i = \delta/i$  it is  $\approx 21.76$  and for  $\mu_i = \sigma/i^2$  it is  $\approx 18.85$ . (Choosing parameters to have density  $\rho = 1/4$  we put  $\nu = 1/10$  for all cases.)

Average waiting times  $t_i, i = 1, \dots, 5$  in the case  $\mu_i = \delta/i$  for various densities are shown in the right panel of Figure 4. For small densities the maximal waiting time  $t_i$  is for  $i = 5$ , while for bigger densities the maximum is for  $i = 3$ . Average waiting times range from  $\approx 13.57$  for  $\rho = 1/10$  through  $\approx 21.76, \approx 50.22, \approx 145.01$  for densities  $1/4, 1/2, 3/4$  respectively, up to  $\approx 441.60$  for density  $\rho = 9/10$ . (Again  $\nu = 1/10$  for all cases.)

### C. $N = 7$

For  $N = 7$  we investigate properties of the system with the density  $\rho = 3/4$ . Parameters are chosen as follows:  $\mu = 1, \nu = 173024/10000$  gives the density  $\rho = 0.7500001621$ ,  $\theta = 1/3$  gives  $\rho = 3/4$  exactly, and  $\mu = 1, \nu := 1000000/1578886$  gives  $\rho = 0.7500002817$ . Distributions of clusters are presented in Figure 5 and average cluster and avalanche sizes in Table VII. Again differences in distributions  $n_i$  are not big, but average

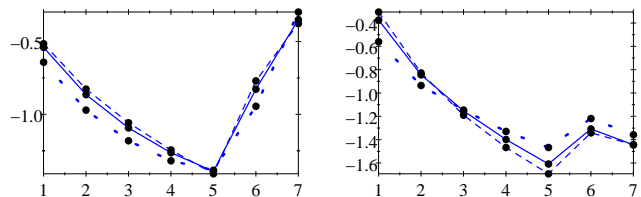


FIG. 5: Plot of the  $\text{Log}_{10}$  of  $n_i$ s (left) and  $n_i^0$ s (right) versus  $i$  for  $N = 7$  in three cases:  $\mu_i = \text{const.}$  (dashed line),  $\mu_i = \delta/i$  (solid line) and  $\mu_i = \sigma/i^2$  (dotted line). Rebound parameters are chosen to have density  $\rho = 3/4$  in all cases (see main text for respective values).

avalanche size differs significantly between considered cases.

The novel property visible in the figure is that the highest probability is for the cluster of maximal size  $i = N$ . Thus, the system prefers merging clusters for high density.

A comparison of the ratios of return times  $R = t_{L \rightarrow L}/t_{1 \rightarrow 1}$  is presented in the right panel of Figure 3, while formulas are presented in the Appendix. In each case the ratio is a rational function of  $t$ , which is equal to 1 for  $t = 0$  and asymptotically  $\sim t^6$  for  $t \rightarrow \infty$ , which supports a Conjecture formulated in Section VII. Table VIII shows that for the cases discussed above, with average density  $\rho = 3/4$ , the highest value of the ratio  $R$  is for  $\mu_i = \delta/i$  and the smallest for  $\mu_i = \text{const.}$  (which does not differ much from the value for  $\mu_i = \delta/i$ ). This is an opposite order comparing to the case with  $\rho = 1/5$  for  $N = 5$  considered above. Thus, for higher densities the automaton prefers more periodic-like behaviour when it is relatively easier to trigger big avalanches.

The size  $N = 7$  is big enough to notice how the actual density of the system (possible values are  $0, \frac{1}{7}, \frac{2}{7}, \frac{3}{7}, \frac{4}{7}, \frac{5}{7}, \frac{6}{7}, 1$ ) is distributed for various average densities. Results are shown in Figure 6. For small densities, like  $\rho = 0.2$ , the maximum is for small  $i$ , that means that big densities and big avalanches are rare. Then, when the density increases, the bell-like shape distribution appears and its maximum is shifted to the bigger values. Next, for densities like 0.6 or bigger, the maximum probability is for biggest possible size  $i = N$  and the most probable state is that with  $\rho = 1$ . To achieve big average density, the system must spend a substantial time being fully occupied. The evolution of such a system consists of two phases: filing up and waiting for avalanche of maximal size, as is described above while discussing the times of return for  $N = 3$ .

	$\mu_i = \text{const.}$	$\mu_i = \delta/i$	$\mu_i = \sigma/i^2$
$\langle i \rangle$	4.274328495	4.385371765	4.736665115
$\langle w \rangle$	5.767461682	4.385371765	2.671314107

TABLE VII: Average cluster size  $\langle i \rangle$  and average avalanche size  $\langle w \rangle$  for three different rebound parameters. Density  $\rho = 3/4$ , the size of the lattice  $N = 7$ .



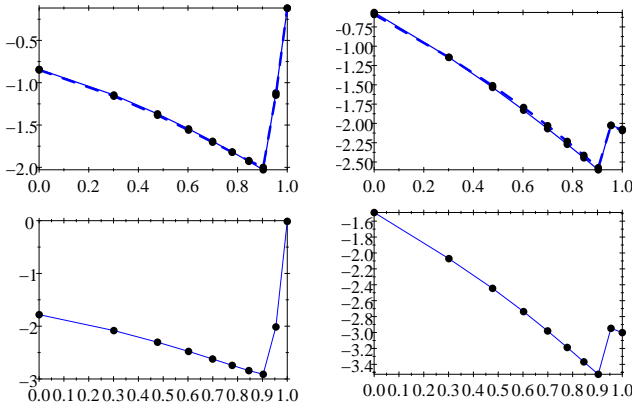


FIG. 8: Plot of the  $\text{Log}_{10}$  of  $n_i$ s and  $n_i^0$  vs.  $\text{Log}_{10}(i)$  for  $N = 10$  in two cases:  $\mu_i = \text{const.}$  (solid line) and  $\mu_i = \delta/i$  (dashed line) – upper panels, and in case  $\mu_i = \delta/i^2$  – lower panels.

tions. In all cases, the assumption of independence of clusters is well satisfied; the respective error  $\Delta$  does not exceed 2%. An approximation for  $\alpha_4^E$  is less than 10% for all cases, but  $\alpha_1^E$  strongly depends on the case (in fact it depends on density, as will be seen below). Approximation formulas for  $\gamma_E$  perform in diversified way –  $\gamma_{AR}$  is better for mid  $i$  terms, while  $\gamma_A$  is better for big  $i$  terms. Nevertheless, both cases provide rather roughly appropriate values. These examples also suggest that for higher densities the system exhibits a periodic-like evolution.

*b. Big densities* In order to investigate evolution of the system with high average density (and strong deviations in actual density) we consider case  $\mu = \text{const}$  with  $\mu_1 = 1/100$  and  $\nu = 1$ , which gives the density  $\rho \approx 0.91$ ,

	$\mu_i \sim 1$	$\mu_i \sim 1/i$	$\mu_i \sim 1/i^2$
$\rho$	0.9145269069	0.9145269069	0.9897960692
$\langle i \rangle$	7.764600567	7.805017612	9.700144892
$\langle w \rangle$	9.346154002	7.805017612	8.33021261
$p_{ss} - 2p_{sq}$	0.00161	0.00464	0.00191
$\frac{\alpha_1^E - \alpha_1^A}{\alpha_1^E}$	0.30898	0.28421	0.31377
$\frac{\alpha_4^E - \alpha_4^A}{\alpha_4^E}$	-0.01511	0.01520	0.00330
$\frac{\gamma_5^E - \gamma_5^A}{\gamma_5^E}$	-0.96763	-0.93825	-1.05131
$\frac{\gamma_5^E - \gamma_5^{AR}}{\gamma_5^E}$	-0.15298	-0.14354	-0.14789
$\frac{\gamma_9^E - \gamma_9^A}{\gamma_9^E}$	0.42749	0.39218	0.38965
$\frac{\gamma_9^E - \gamma_9^{AR}}{\gamma_9^E}$	0.80211	0.78888	0.80019
$t_{1 \rightarrow 1}$	119.18	123.60 <sup>a</sup>	1002.44
$t_{L \rightarrow L} / t_{1 \rightarrow 1}$	1.1066	1.1339	1.0277

<sup>a</sup>The system stays in fully occupied state  $1/\mu_{10} \approx 107.5$ , which is longer than 100 as in  $\mu = \text{const.}$  case (previous column). The respective average times for filling up the lattice are  $\approx 19$  and  $\approx 16$ .

TABLE X: Three cases with "big"  $\rho$  for the size of the lattice  $N = 10$  (see main text for details).

and case  $\delta/i$  with  $\mu_1 = 4673077001/5 * 10^{10} \approx 0.093$  and  $\nu = 1$  to obtain the same density (with 10 digits accuracy) for comparison. Also we consider case of  $\sigma/i^2$  with  $\mu_1 = 1/10$  and  $\nu = 1$  which gives the density  $\rho \approx 0.99$ . The results are presented in Figure 8 and Table X.

Plots of respective distributions for  $\mu_i \sim 1/i$  and  $\mu_i \sim 1$  are overlapping each other. For relatively small size  $N = 10$ , fixing the average density of the system strongly determines distributions, making the dependence on rebound parameters not essential. Their influence becomes more visible for larger sizes  $N$  of the lattice. In case of high density, the system just spend much time being fully occupied.

For high densities, the assumption of independence of clusters is well satisfied; the respective error  $\Delta$  does not exceed 0.5%. An approximation for  $\alpha_4^E$  is fairly good ( $\approx 1.5\%$  or less), but  $\alpha_1^E$  has only accuracy  $\approx 30\%$ . Approximation formula for  $\gamma_{AR}$  is much better for mid  $i$  terms (though giving only  $\approx 15\%$  accuracy), while  $\gamma_A$  is better for big  $i$  terms ( $\approx 40\%$ ). Thus, for high density cases the proposed set of equations for  $n_i$ s does not reproduce actual distribution. Note, however, that there are other exact equations valid for any density.

The parameter  $t_{L \rightarrow L} / t_{1 \rightarrow 1}$  for  $\mu_i \sim 1/i$  case is bigger than for  $\mu_i \sim 1$  case (both cases have the same "big" density), which agrees with the results for  $N = 7$  with  $\rho = 3/4$  presented in Table VIII.

*c. Small densities* To present system behaviour in small average density we choose  $\mu_1 = 1$  and  $\nu = 1/10$  for case  $\mu = \text{const}$  - it gives density  $\rho \approx 0.08$ . Then for the remaining two cases we have the same density  $\rho \approx 0.01$  (with 10 digits accuracy), with the following parameters:  $\mu_1 = 1$  and  $\nu = 50000000/4798952601 \approx 0.01$  - for case  $\delta/i$  and  $\mu_1 = 1$  and  $\nu = 1/100$  for case  $\sigma/i^2$ . The results are presented in Figure 9 and Table XI.

For small densities assumption of independence of clusters is well satisfied. In general, all proposed approxima-

	$\mu_i \sim 1$	$\mu_i \sim 1/i$	$\mu_i \sim 1/i^2$
$\rho$	0.0779280356	0.01031150521	0.01031150521
$\langle i \rangle$	1.09149321	1.02083788	1.041894016
$\langle w \rangle$	1.183235221	1.02083788	1.020408163
$p_{ss} - 2p_{sq}$	$6.9231 * 10^{-5}$	$6.4609 * 10^{-4}$	$3.5663 * 10^{-3}$
$\frac{\alpha_1^E - \alpha_1^A}{\alpha_1^E}$	$1.7483 * 10^{-5}$	$2.7693 * 10^{-7}$	$1.0585 * 10^{-6}$
$\frac{\alpha_4^E - \alpha_4^A}{\alpha_4^E}$	0.14229	0.16313	0.16274
$\frac{\gamma_5^E - \gamma_5^A}{\gamma_5^E}$	0.0009069	0.0020519158	0.0040100
$\frac{\gamma_5^E - \gamma_5^{AR}}{\gamma_5^E}$	0.0009101	0.0020519262	0.0040124
$\frac{\gamma_9^E - \gamma_9^A}{\gamma_9^E}$	0.09615	0.01473	0.00606
$\frac{\gamma_9^E - \gamma_9^{AR}}{\gamma_9^E}$	0.12138	0.02356	0.03305
$t_{1 \rightarrow 1}$	22.32	106.35	110.57
$t_{L \rightarrow L} / t_{1 \rightarrow 1}$	2220903488.0	$1.666292752 * 10^{14}$	$9971770329.0$
	$\sim 2 * 10^{10}$	$\sim 2 * 10^{14}$	$\sim 1 * 10^{11}$

TABLE XI: Three cases with "small"  $\rho$  for the size of the lattice  $N = 10$  (see main text for details).

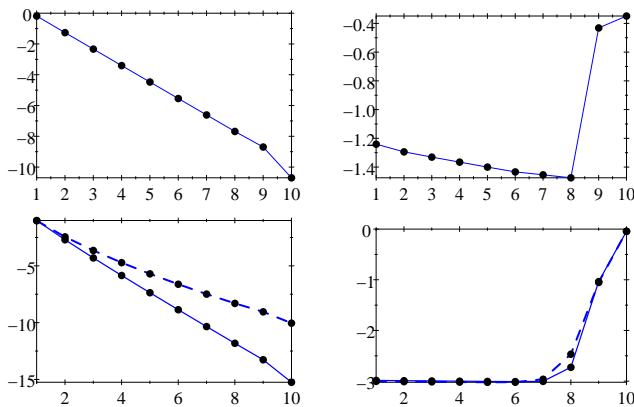


FIG. 9: Plot of the  $\text{Log}_{10}$  of  $n_i$ s and  $n_i^0$  for  $N = 10$  in case  $\mu_i = \text{const.}$  – upper line, and in two cases:  $\mu_i = \delta/i$  (solid line) and  $\mu_i = \delta/i^2$  (dashed line) – lower line.

tions are fairly good. An approximation for  $\alpha_4^E$  is the worst; its accuracy is only  $\approx 15\%$ . As previously, approximation formula for  $\gamma_A$  is better than  $\gamma_{AR}$  for big  $i$  terms, but it appears that for mid  $i$  terms both formulas give almost the same values (because  $n_i$ s decrease rapidly). Thus, for small densities the set of equations for  $n_i$ s can be used to reproduce the actual distribution.

It is very improbable to find the lattice fully occupied for small average densities, which is reflected in high values of the parameter  $R = t_{L \rightarrow L} / t_{1 \rightarrow 1}$ . The parameter  $R$  for  $\mu_i \sim 1/i$  case is bigger than its for  $\mu_i \sim 1/i^2$  case (both cases have the same "small" density), which agrees with the results for  $N = 5$  with  $\rho = 1/4$  presented in Table VI.

## VII. CONCLUSIONS

In this article we investigated in detail a finite version of one-dimensional non-equilibrium dynamical system – Random Domino Automaton. It is a simple, slowly driven system with avalanches. The advantage of RDA (comparing to Drossel-Schwabl model) is the dependence of rebound parameters on the size of a cluster. This crucial extension allows for producing a wider class of distributions by the automaton, as well as leads to several exact formulas. Exponential type and inverse-power type distributions of clusters were studied in [1]; the present work examines also V-shape distributions and quasi-periodic like behavior.

Detailed analysis of finite RDA, including finite size effects, extends and explains the previously obtained results for RDA. Moreover, we also analyzed approximations made when deriving equations for the stationary state of the automaton. This allows for the following conclusions.

The balance of  $\rho$  equation (4) and the balance of  $N$  equations (9) are exact – their forms incorporate all correlations present in the system. The first one has a form

independent of the size of the lattice  $N$ , thus it is exactly the same as for RDA. The second one contains correction for finite size effect, namely a term  $(2n_R - n_{N-1})$ , which replaces the term  $2n$  for RDA. When  $n_{N-1}$  and  $n_N$  are negligible, these two terms coincide. For finite RDA, balance of  $n_i$ s equations (18)-(22) contains two extra equations, for  $i = N - 1$  and  $i = N$ , comparing to those for RDA. The first (for  $n_1$ ) and the last (for  $n_N$ ) are exact. Note that all those equations are written for rebound parameter  $\mu = \mu(i)$  being a function of cluster size and  $\nu$  being a constant.

The most remarkable special case is when  $\mu = \delta/i$ , when any cluster has the same probability to be removed as an avalanche independently of its size  $i$ . It appears that the system depends on a single parameter  $\theta = \delta/\nu$ , or equivalently, due to neat exact formula (eq. (33))

$$\rho = \frac{1}{1 + \theta},$$

the properties of the system may be characterized by the value of the average density. Note that the above expression does not depend on the size  $N$ , and is the same as for RDA. This specialization leads to more neat formulas, like the equation for  $n_R$  (eq. (35))

$$n_R = N \frac{\theta}{(\theta + 1)(\theta + 2)}.$$

Note again that it has the same form as for RDA, except that  $n$  is replaced by  $n_R$  ( $n = n_R + n_N$ ). Summarizing, the model allows to derive a number of explicit dependencies, as shown in Sections III and IV.

The Random Domino Automaton defines a discrete time Markov process of order 1 and, in principle, may be solved exactly. However, it turns out that computations are fairly complex and exact formulas are long, as visible from examples presented in the Appendix. Also, the exact numerical values are in the form of big numbers – in every considered example ( $N = 3, 4, 5, 6, 7, 10$ ) significantly big prime numbers were encountered. For example, for the simplest possible rebound parameters ( $\mu = 1$  and  $\nu = 1$ ) the exact value of denominators of probabilities of states for  $N = 10$  (see Table XIV) is a 65-digit integer. Its prime factorization (presented in the Appendix) contains a 56-digit integer, which cannot be simplified with numerators. Thus, the usefulness of Markov chains for finding both formulas and values  $n_i$ s is limited in practice.

Nevertheless, Markov chains framework leads to interesting results concerning analysis of times of recurrence for specific states. A return time to the state with density  $\rho = 1$  (equation (50))

$$t_{L \rightarrow L} = 1/\mu_N + \hat{\tau}_1,$$

consists of two parts: waiting of fully occupied lattice for triggering a maximal avalanche and "loading" time, when the lattice is filled up, respectively. If the average density of the system is small, the second time is very long. The

formula is more interesting for systems with relatively big average density, when the "loading" time is comparable to waiting time for triggering the biggest avalanche. Such a system exhibits a periodic like behavior. Dividing the waiting time  $t_{L \rightarrow L}$  by the waiting time  $t_{1 \rightarrow 1}$  (given by equation (49)) one has the following measure of quasi-periodicity

$$R = t_{L \rightarrow L}/t_{1 \rightarrow 1} = t_{1 \rightarrow L \rightarrow 1}/t_{1 \rightarrow 1}.$$

If  $R = 1$  then the system is periodic.

Several considered examples lead to the following conjecture concerning the coefficient  $R$ .

**Conjecture.** The ratio of return times  $t_{L \rightarrow L}/t_{1 \rightarrow 1}$  as a function of  $t$  being the ratio of constants from rebound parameters ( $\mu/\nu$ ,  $\delta/\nu$ ,  $\sigma/\nu$ ) are rational functions of  $t$ ,  $f(t) = t_{L \rightarrow L}/t_{1 \rightarrow 1}$  with the following properties for any size  $N$  of the system

$$f(t=0) = 1, \quad (76)$$

$$\lim_{t \rightarrow \infty} \frac{f(t)}{t^{N-1}} = \text{const.} \quad (77)$$

The conjecture relates the size of the system  $N$  with asymptotic behavior of ratio of waiting times.

There are big fluctuations (variations of actual density) during the evolution of systems with relatively big average densities. If the system is likely to achieve a fully occupied state, the next state is an empty state, and the variations in density are maximal. Nevertheless, some parameters of stationary state (more precisely, statistically stationary state) satisfy exact equations, as shown above. For big average densities, the system fluctuates within the whole possible range, and cannot be thought of as having approximately stationary values during the evolution. This aspect is easy to be overlooked (see [14]).

It is argued in the Appendix that no exact equations for  $n_i$ s exist for the size  $N \geq 5$ . Thus, to have compact equations for  $n_i$ s, some approximation formulas are proposed. The first general conclusion from the examples is that the approximations are acceptable for small densities, but for big densities the errors are substantial. The main reason is that for big densities correlations become more important and fluctuations makes actual values of the parameters substantially different from their stationary values, which are present in the formulas. These properties are particularly severe for small sizes of the system, where every avalanche changes the actual density considerably.

Table XII presents a dependence of a relative error of  $\alpha_1^E$  with respect to  $\alpha_1^A$  on size  $N$  of the system. For bigger  $N$  the accuracy of approximation is growing, which corresponds well with the remark in the last paragraph.

It can be noticed from the distributions of  $n_i$ s of examples presented above that all  $n_i$ s except of the last two (namely  $n_{N-1}$  and  $n_N$ ) are placed on one "regular" curve, while the last two deviate from it. It may be regarded as a (correction of) finite size effect. Also in the respective set of equations (18)-(22), the last two (for

$N$	$\alpha_1^E = \frac{2n_2}{n_1}$	$\alpha_1^A = \left(1 - \frac{n_1^0}{n_R}\right)$	$\frac{\alpha_1^E - \alpha_1^A}{\alpha_1^E}$	$\rho$
3	1.33(3)	0.6	0.55	$\approx 0.3462$
4	0.66(6)	$\approx 0.6316$	$\approx 0.053$	0.32(32)
5	$\approx 0.6829$	$\approx 0.6565$	$\approx 0.039$	$\approx 0.3139$
6	$\approx 0.685296$	$\approx 0.669232$	$\approx 0.023$	$\approx 0.3102$
7	$\approx 0.685523$	$\approx 0.675066$	$\approx 0.015$	$\approx 0.3086$
10	$\approx 0.685436$	$\approx 0.679205^a$	$\approx 0.0091$	$\approx 0.3076$
4000 <sup>b</sup>	$\approx 0.677$	$\approx 0.677$	—	$\approx 0.3076$

<sup>a</sup> $(1 - n_1^0/n) \approx 0.679229$

<sup>b</sup>Results from [1]

TABLE XII: Comparison of  $\alpha_1^E$  with  $\alpha_1^A$  for  $N = 3, 4, 5, 6, 7$  and 10 for parameters  $\mu = 1$  and  $\nu = 1$ . The last line presents value of  $\alpha_1^A$  for  $N = 4000$  obtained from simulations and equations (respectively) in [1].

$i - N - 1$  and  $i = N$ ) have a form different from the previous ones. Thus, neglecting the size restriction, which in fact ignores the last two equations, is justified when the deviations of the last two  $n_i$ s from the "regular" curve are not big. That happens for small densities.

It appears also that for index  $i$  in his middle range of values an approximation formula  $\gamma_{AR}$  works better than  $\gamma_A$ , in spite of the fact that it looks to be more rough approximation. For distribution of  $n_i$ s vanishing rapidly (i.e., for small densities) both give comparable results.

All this justifies the form of equations for  $n_i$ s presented in [1] as valid for small densities. A detailed examination of the RDA for big densities requires further investigations.

This article explores properties of FRDA in order prepare to modeling of real data. In this context, among others, formulas for waiting times can be used. We emphasize also a formula (53)

$$t_{av} = \frac{\langle w \rangle + 1}{1 - P_r},$$

which relates the measure of scattering (dissipation) of balls  $P_r$  with the average size of avalanche  $\langle w \rangle$  and average time between any two consecutive avalanches  $t_{av}$ , which are a priori measurable quantities.

The Random Domino Automaton proved to be a stochastic dynamical system with interesting mathematical structure. It may be viewed as extension of Drossel-Schwabl model, and we showed that this is a substantial generalization with a wide range of novel properties. We expect it can also be applied to natural phenomena, including earthquakes and forest-fires. This is our aim for the future work.

#### Appendix. Exact equations for $N = 3, 4$ and their non-existence for $n \geq 5$

For arbitrary size  $N$ , there are four exact equations: balance of  $\rho$  - equation (4), balance of  $n$  - equation (9), for  $n_1$  - equation (18) and for  $n_N$  - equation (22).

state number	example <sup>a</sup>	multiplicity	contrib. to
1	↔           ↔	1	$n_4^0$
2	↔         •   ↔	4	$n_1, n_3^0$
3	↔       • •   ↔	4	$n_3, n_2^0$
4	↔     •   •   ↔	2	$n_1, n_1^0$
5	↔     • • •   ↔	4	$n_3, n_1^0$
6	↔   • • • •   ↔	1	$n_4$

<sup>a</sup>Other states differ by shifts.

TABLE XIII: States for the size of the lattice  $N = 4$ .

**Size  $N = 3$ .** Equation for  $n_2$  is of the form (21), namely

$$n_2 = \frac{1}{2\frac{\mu_1}{\nu} + 1} (2n_1\alpha_1^E + n_1^0\gamma_2^E).$$

In this case the only companion to single one-cluster is an empty two-cluster (see state 2 in Tab.I), hence

$$\alpha_1^E = 1 \quad \text{and} \quad \gamma_2^E = 0.$$

Thus, we arrived at the exact form of the equation for  $n_2$ .

**Size  $N = 4$ .** All states of the automaton and their labels are presented in Tab.XIII. Equation for  $n_2$  is of the form (19)

$$n_2 = \frac{2}{2\frac{\mu_2}{\nu} + 2} n_1\alpha_1^E,$$

where to  $\alpha^E$  contributes only state 2, not state 4. Hence

$$\alpha_1^E = \frac{p_2}{p_2 + 2p_4} = \left(1 - \frac{2p_4}{n_1}\right) = \left(1 - \frac{n_1^0 - n_3}{n_1}\right),$$

where  $p_i$  is probability of state  $i$ . Thus  $\alpha_1^E$  is expressed as function of  $n_i$ s and  $n_1^0$ . The equation for  $n_3$  is of the form (21)

$$n_3 = \frac{1}{3\frac{\mu_3}{\nu} + 1} (2n_2\alpha_2^E + n_1^0\gamma_3^E).$$

In this case

$$\alpha_2^E = 1,$$

because only state 3 contributes. The state 4 (and not state 5) contributes to  $\gamma_3^E$ , therefore

$$\gamma_3^E = \frac{2p_4}{2p_4 + p_5} = \left(1 - \frac{p_5}{n_1^0}\right) = \left(1 - \frac{n_3}{n_1^0}\right).$$

This completes the task of writing exact equations for  $N = 4$ .

**Size  $N = 5$ .** States and their labels are presented in Tab.II. In this case, the coefficients are as follows

$$\alpha_2^E = \frac{p_2 + p_4}{n_1}, \quad \gamma_3^E = \frac{p_4 - p_6 - n_4}{n_1^0},$$

$$\alpha_3^E = \frac{p_3}{n_2}, \quad \gamma_4^E = \frac{p_6 - p_4 - n_4}{n_1^0}.$$

Summing up the probabilities contributing to  $n_1^0, n_1$  and  $n_2$  one obtains

$$n_1^0 = p_4 + 2p_6 + n_4, \quad (78)$$

$$n_1 = p_2 + 2p_4 + p_6, \quad (79)$$

$$n_2 = p_3 + p_6. \quad (80)$$

The set cannot be solved for  $p_2, p_3, p_4, p_6$ . Since there are no more equations for those coefficients, respective  $\alpha$ s and  $\gamma$ s cannot be expressed as functions of  $n_i$ s only in an exact manner.

**Sizes bigger than 5.** An argument for non-existence of exact set of equations (18)-(22), i.e., non-existence of exact formulas for  $\alpha_i^E$ s and  $\gamma_i^E$ s as functions of  $n_i$ s and  $n_1^0$  is based on the same impossibility of solving equations as presented above.

An increase of size of a grid  $N$  by 1 results in an increase of the set of  $n_1, n_2, \dots$  by one and much bigger increase of the number of states. An analog of the set of equations (78)-(80) will contain much more probabilities of states  $p_1, p_2, \dots$ , on the right hand side – there will be more states containing 1-clusters, 2-clusters and so on, and contributing to  $n_1, n_2, \dots$  respectively. Thus, it is impossible to express those probabilities of states as functions of  $n_1^0, n_1, n_2, \dots$  only. As a consequence, there are no general exact formulas for  $\alpha_i^E$ s and  $\gamma_i^E$ .

## Appendix. Formulas

The return times for  $N = 5$  for general values of the parameters  $\mu_1, \mu_2, \mu_3, \mu_4, \mu_5$  and  $\nu$  are

$$t_{1 \rightarrow 1} = \frac{1}{\nu} + \frac{1}{\mu_5(4\mu_4 + \nu)(3\mu_3 + 2\nu)(2m\mu_1^3\mu_2 + 2\mu_1^3\nu + 4\mu_1^2\mu_2^2 + 17\mu_1^2\mu_2\nu + 13\mu_1^2\nu^2 + 14\mu_1\mu_2^2\nu + 43\mu_1\mu_2\nu^2 + 33\mu_1\nu^3 + 16\mu_2^2\nu^2 + 42\mu_2\nu^3 + 36\nu^4)} \times$$

$$(48\mu_1\nu^5 + 60\mu_2\nu^5 + 54\mu_3\nu^5 + 750\mu_5\nu^5 + 72\nu^6 + 8\mu_1^2\nu^4 + 8\mu_2^2\nu^4 + 20\mu_1\mu_2\nu^4 + 12\mu_1\mu_3\nu^4 + 24\mu_2\mu_3\nu^4 +$$

$$560\mu_1\mu_5\nu^4 + 760\mu_2\mu_5\nu^4 + 720\mu_3\mu_5\nu^4 + 1560\mu_4\mu_5\nu^4 + 100\mu_1^2\mu_5\nu^3 + 160\mu_2^2\mu_5\nu^3 + 40\mu_1\mu_2^2\mu_5\nu^2 + 20\mu_1^2\mu_2\mu_5\nu^2 +$$

$$60\mu_1^2\mu_3\mu_5\nu^2 + 240\mu_1^2\mu_4\mu_5\nu^2 + 150\mu_2^2\mu_3\mu_5\nu^2 + 480\mu_2^2\mu_4\mu_5\nu^2 + 340\mu_1\mu_2\mu_5\nu^3 + 390\mu_1\mu_3\mu_5\nu^3 + 1280\mu_1\mu_4\mu_5\nu^3 +$$

$$645\mu_2\mu_3\mu_5\nu^3 + 1840\mu_2\mu_4\mu_5\nu^3 + 1800\mu_3\mu_4\mu_5\nu^3 + 240\mu_1\mu_2^2\mu_3\mu_4\mu_5 + 120\mu_1^2\mu_2\mu_3\mu_4\mu_5 + 285\mu_1\mu_2\mu_3\mu_5\nu^2 + 60\mu_1\mu_2^2\mu_3\mu_5\nu +$$

$$30\mu_1^2\mu_2\mu_3\mu_5\nu + 960\mu_1\mu_2\mu_4\mu_5\nu^2 + 160\mu_1\mu_2^2\mu_4\mu_5\nu + 80\mu_1^2\mu_2\mu_4\mu_5\nu + 1320\mu_1\mu_3\mu_4\mu_5\nu^2 + 240\mu_1^2\mu_3\mu_4\mu_5\nu + 2100\mu_2\mu_3\mu_4\mu_5\nu^2 +$$

$$600\mu_2^2\mu_3\mu_4\mu_5\nu + 1140\mu_1\mu_2\mu_3\mu_4\mu_5\nu),$$

$$t_{L \rightarrow L} = \frac{1}{\mu_5} + \frac{1}{2\nu^5(4\mu_1^2+10\mu_1\mu_2+24\mu_1\nu+6\mu_3\mu_1+4\mu_2^2+30\mu_2\nu+12\mu_3\mu_2+36\nu^2+27\mu_3\nu)} \times (626\mu_1\nu^5+844\mu_2\nu^5+828\mu_3\nu^5+1848\mu_4\nu^5+822\nu^6+126\mu_1^2\nu^4+4\mu_1^3\nu^3+192\mu_2^2\nu^4+8\mu_1^2\mu_2^2\nu^2+426\mu_1\mu_2\nu^4+489\mu_1\mu_3\nu^4+1544\mu_1\mu_4\nu^4+771\mu_2\mu_3\nu^4+2176\mu_2\mu_4\nu^4+2232\mu_3\mu_4\nu^4+68\mu_1\mu_2^2\nu^3+54\mu_1^2\mu_2\nu^3+4\mu_1^3\mu_2\nu^2+99\mu_1^2\mu_3\nu^3+6\mu_1^3\mu_3\nu^2+344\mu_1^2\mu_4\nu^3+16\mu_1^3\mu_4\nu^2+198\mu_2^2\mu_3\nu^3+608\mu_2^2\mu_4\nu^3+48\mu_1^2\mu_2^2\mu_3\mu_4+102\mu_1\mu_2^2\mu_3\nu^2+81\mu_1^2\mu_2\mu_3\nu^2+12\mu_1^2\mu_2^2\mu_3\nu+272\mu_1\mu_2^2\mu_4\nu^2+216\mu_1^2\mu_2\mu_4\nu^2+32\mu_1^2\mu_2^2\mu_4\nu+396\mu_1^2\mu_3\mu_4\nu^2+792\mu_2^2\mu_3\mu_4\nu^2+24\mu_1^3\mu_2\mu_3\mu_4+414\mu_1\mu_2\mu_3\nu^3+6\mu_1^3\mu_2\mu_3\nu+1304\mu_1\mu_2\mu_4\nu^3+16\mu_1^3\mu_2\mu_4\nu+1716\mu_1\mu_3\mu_4\nu^3+24\mu_1^3\mu_3\mu_4\nu+2604\mu_2\mu_3\mu_4\nu^3+1656\mu_1\mu_2\mu_3\mu_4\nu^2+408\mu_1\mu_2^2\mu_3\mu_4\nu+324\mu_1^2\mu_2\mu_3\mu_4\nu).$$

Their ratio is

$$t_{L \rightarrow L}/t_{1 \rightarrow 1} = \frac{(4\mu_4+\nu)*(3\mu_3+2\nu)*(2\mu_3^2\mu_2+2\mu_1^3\nu+4\mu_1^2\mu_2^2+17\mu_1^2\mu_2\nu+13\mu_1^2\nu^2+14\mu_1\mu_2^2\nu+43\mu_1\mu_2\nu^2+33\mu_1\nu^3+16\mu_2^2\nu^2+42\mu_2\nu^3+36\nu^4)}{2\nu^4(4\mu_1^2+10\mu_1\mu_2+24\mu_1\nu+6\mu_3\mu_1+4\mu_2^2+30\mu_2\nu+12\mu_3\mu_2+36\nu^2+27\mu_3\nu)}.$$

Average waiting times  $t_i$  for avalanche of size  $i$  in case  $\mu_i = \delta/i$ , where  $\delta = const.$  and  $t := \delta/\nu$ , for  $N = 5$ , are

$$t_1 = \frac{4t^5 + 48t^4 + 237t^3 + 603t^2 + 762t + 360}{\nu t^2(4t^3 + 28t^2 + 69t + 60)}, \quad (81)$$

$$t_2 = \frac{4t^5 + 48t^4 + 237t^3 + 603t^2 + 762t + 360}{2\nu t^2(4t^2 + 16t + 15)}, \quad (82)$$

$$t_3 = \frac{4t^6 + 56t^5 + 333t^4 + 1077t^3 + 1968t^2 + 1884t + 720}{2\nu t^2(10t^2 + 31t + 18)}, \quad (83)$$

$$t_4 = \frac{4t^7 + 60t^6 + 389t^5 + 1410t^4 + 3045t^3 + 3852t^2 + 2604t + 720}{8\nu t^2(7t^2 + 24t + 18)}, \quad (84)$$

$$t_5 = \frac{4t^7 + 60t^6 + 389t^5 + 1410t^4 + 3045t^3 + 3852t^2 + 2604t + 720}{8\nu t(7t^2 + 24t + 18)}. \quad (85)$$

The ratio of return times for  $N = 7$  for three cases:  
for  $\mu = const.$

$$t_{L \rightarrow L}/t_{1 \rightarrow 1} = (5184000t^{16} + 90633600t^{15} + 734038560t^{14} + 3656624904t^{13} + 12543798852t^{12} + 31435490078t^{11} + 59579986661t^{10} + 87223274254t^9 + 99846813214t^8 + 89833419890t^7 + 63379753809t^6 + 34652851894t^5 + 14319281196t^4 + 4279417752t^3 + 859191840t^2 + 101520000t + 5184000)/(5184000t^{10} + 60393600t^9 + 306948960t^8 + 896350104t^7 + 1664901648t^6 + 2053477662t^5 + 1700206878t^4 + 930252240t^3 + 320428800t^2 + 62380800t + 5184000),$$

for  $\mu_i/\nu = \theta/i$

$$t_{L \rightarrow L}/t_{1 \rightarrow 1} = (576t^{16} + 16800t^{15} + 229696t^{14} + 1956752t^{13} + 11645844t^{12} + 51472058t^{11} + 175326610t^{10} + 471411274t^9 + 1015867913t^8 + 1768373403t^7 + 2486683328t^6 + 2797983376t^5 + 2465006400t^4 + 1636404624t^3 + 767257920t^2 + 225504000t + 31104000)/(76032t^{10} + 1450368t^9 + 12336072t^8 + 61572600t^7 + 199652130t^6 + 439389384t^5 + 664690536t^4 + 682575840t^3 + 455457600t^2 + 178329600t + 31104000),$$

and for  $\mu = \sigma/i^2$

$$t_{L \rightarrow L}/t_{1 \rightarrow 1} = (27000t^{16} + 1648350t^{15} + 46021545t^{14} + 781598610t^{13} + 9060806565t^{12} + 76286696592t^{11} + 484749056302t^{10} + 2385421175676t^9 + 9253317988496t^8 + 28615082281632t^7 + 70836261328608t^6 + 139636245477312t^5 + 215233793554176t^4 + 250177275371520t^3 + 205696375603200t^2 + 106205478912000t + 25798901760000)/(1032264000t^{10} + 28816738200t^9 + 362493838440t^8 + 2695926522960t^7 + 13095290178720t^6 + 43360671643200t^5 + 99111840724224t^4 + 154547465674752t^3 + 157566016143360t^2 + 95025954816000t + 25798901760000).$$

The exact value of  $\alpha_4^E$  for  $N = 10$ :

$$\alpha_4^E = \frac{2v_{20} + v_{43} + 2v_{44} + 2v_{45} + v_{46} + v_{72} + 2v_{73} + v_{74} + v_{77} + 2v_{79} + v_{95} + v_{96}}{2(v_{20} + v_{43} + v_{44} + v_{45} + v_{46} + v_{72} + v_{73} + v_{74} + v_{77} + v_{78} + v_{79} + v_{95} + v_{96} + v_{98} + v_{99} + 2v_{106})}.$$

A prime factorization of the common factor of probabilities of states of FRDA for  $N = 10$  (presented in Table XIV) for rebound parameters  $\mu = 1$  and  $\nu = 1$ :

$$2^2 * 3^2 * 607 * 66617 * 35622218878023086289926346229321892786614786277415883867.$$

The biggest prime has 56 digits.

	states	probability	sym		states	probability	sym
1		0.05402	( <sup>1</sup> )	55	• • • • • • • •	0.00399	52
2		0.13914		56	• • • • • • • •	0.00441	51
3		0.06060		57	• • • • • • • •	0.00422	59
4		0.04841		58	• • • • • • • •	0.00370	
5		0.04075		59	• • • • • • • •	0.00422	57
6		0.03777		60	• • • • • • • •	0.00348	61
7		0.01853	( <sup>5</sup> )	61	• • • • • • • •	0.00348	60
8		0.03074		62	• • • • • • • •	0.00401	
9		0.02256	14	63	• • • • • • • •	0.00355	66
10		0.01807	13	64	• • • • • • • •	0.00344	65
11		0.01657	12	65	• • • • • • • •	0.00344	64
12		0.01657	11	66	• • • • • • • •	0.00355	63
13		0.01807	10	67	• • • • • • • •	0.00066	( <sup>2</sup> )
14		0.02256	9	68	• • • • • • • •	0.00492	
15		0.01744		69	• • • • • • • •	0.00355	71
16		0.01450	18	70	• • • • • • • •	0.00308	
17		0.01371		71	• • • • • • • •	0.00355	69
18		0.01450	16	72	• • • • • • • •	0.00313	74
19		0.01252		73	• • • • • • • •	0.00256	
20		0.01641		74	• • • • • • • •	0.00313	72
21		0.01168	25	75	• • • • • • • •	0.00303	
22		0.00926	24	76	• • • • • • • •	0.00122	( <sup>5</sup> )
23		0.00864		77	• • • • • • • •	0.00266	79
24		0.00926	22	78	• • • • • • • •	0.00277	
25		0.01168	21	79	• • • • • • • •	0.00266	77
26		0.01075		80	• • • • • • • •	0.00246	85
27		0.00808		81	• • • • • • • •	0.00249	84
28		0.00372	( <sup>5</sup> )	82	• • • • • • • •	0.00236	83
29		0.00825	38	83	• • • • • • • •	0.00236	82
30		0.00697	37	84	• • • • • • • •	0.00249	81
31		0.00703	35	85	• • • • • • • •	0.00246	80
32		0.00857		86	• • • • • • • •	0.00228	
33		0.00663	36	87	• • • • • • • •	0.00236	
34		0.00612		88	• • • • • • • •	0.00224	
35		0.00703	31	89	• • • • • • • •	0.00111	( <sup>5</sup> )
36		0.00663	33	90	• • • • • • • •	0.00279	
37		0.00697	30	91	• • • • • • • •	0.00219	92
38		0.00825	29	92	• • • • • • • •	0.00219	91
39		0.00656		93	• • • • • • • •	0.00195	94
40		0.00590		94	• • • • • • • •	0.00195	93
41		0.00290	( <sup>5</sup> )	95	• • • • • • • •	0.00186	96
42		0.00893		96	• • • • • • • •	0.00186	95
43		0.00632	46	97	• • • • • • • •	0.00194	
44		0.00510	45	98	• • • • • • • •	0.00178	99
45		0.00510	44	99	• • • • • • • •	0.00178	98
46		0.00632	43	100	• • • • • • • •	0.00174	
47		0.00563	50	101	• • • • • • • •	0.00167	
48		0.00424	49	102	• • • • • • • •	0.00176	
49		0.00424	48	103	• • • • • • • •	0.00164	
50		0.00563	47	104	• • • • • • • •	0.00152	
51		0.00441	56	105	• • • • • • • •	0.00147	
52		0.00399	55	106	• • • • • • • •	0.00073	( <sup>5</sup> )
53		0.00463		107	• • • • • • • •	0.00142	
54		0.00376		108	• • • • • • • •	0.00014	( <sup>1</sup> )

TABLE XIV: All states for the size of the lattice  $N = 10$ . The probabilities are for the case  $\mu = 1$  and  $\nu = 1$ . States which differ by mirror symmetry are indicated in the column with label 'sym'. Values in parenthesis indicate smaller than 10 translational symmetry.



### Acknowledgement

The author would like to express his gratitude to Professors Zbigniew Czechowski, Adam Doliwa and Maciej Wojtkowski for inspiring comments and discussions.

---

- 
- [1] M. Bialecki and Z. Czechowski. Analytic approach to stochastic cellular automata: exponential and inverse power distributions out of random domino automaton. [arXiv:1009.4609 \[nlin.CG\]](#), 2010.
  - [2] B. Drossel and F. Schwabl. Self-Organized Critical Forest-Fire Model. *Phys. Rev. Lett.*, 69:1629–1632, 1992.
  - [3] B. Drossel, S. Clar, and F. Schwabl. Exact Results for the One-Dimensional Self-Organized Critical Forest-Fire Model. *Phys. Rev. Lett.*, 71:3739–3742, 1993.
  - [4] B. D. Malamud, G. Morein, and D. L. Turcotte. Forest Fires: An Example of Self-Organized Critical Behavior. *Science*, 281:1840–1842, 1998.
  - [5] M. Bialecki. Random domino automaton: from avalanches to rebound parameters. in prep., 2012.
  - [6] Z. Czechowski and M. Bialecki. Three-level description of the domino cellular automaton. *J. Phys. A: Math. Theor.*, 45:155101, 2012.
  - [7] Z. Czechowski and M. Bialecki. Ito equations out of domino cellular automaton with efficiency parameters. *Acta Geophys.*, 60(3):846–857, 2012.
  - [8] M. Bialecki. Motzkin numbers out of random domino automaton. [arXiv:1102.0437 \[math-ph\]](#), 2011.
  - [9] D. Weatherley. Recurrence Interval Statistics of Cellular Automaton Seismicity Models. *Pure Appl. Geophys.*, 163:1933–1947, 2006.
  - [10] T. Parsons. Monte Carlo method for determining earthquake recurrence parameters from short paleoseismic catalogs: Example calculations for california. *J. Geophys. Res.*, 113:B03302 (14pp), 2008.
  - [11] M. Vazquez-Prada, A. Gonzalez, J. B. Gomez, and A. F. Pacheco. A minimalist model of characteristic earthquakes. *Nonlinear Processes in Geophysics*, 9:513–519, 2002.
  - [12] A. Tejedor, S. Ambroj, J. B. Gomez, and A. F. Pacheco. Predictability of the large relaxations in a cellular automaton model. *J. Phys. A: Math. Theor.*, 41:375102 (16pp), 2008.
  - [13] M. Bialecki and Z. Czechowski. On a simple stochastic cellular automaton with avalanches: simulation and analytical results. In V. De Rubeis, Z. Czechowski, and R. Teisseyre, editors, *Synchronization and triggering: from fracture to earthquake processes*, pages 63–75. Springer, 2010.
  - [14] M. Paczuski and P. Bak. Theory of the one-dimensional forest-fire model. *Phys. Rev. E*, 48:R3214–R3216, 1993.